0026-895X/00/030576-13$3.00/0

MOLECULAR PHARMACOLOGY, **57**:576–588 (2000).

Cloned Human Aquaporin-1 Is a Cyclic GMP-Gated Ion Channel

TODD L. ANTHONY, HEDDWEN L. BROOKS, DANIELA BOASSA, SERGEY LEONOV, GINA M. YANOCHKO, JOHN W. REGAN, and ANDREA J. YOOL

Departments of Physiology (H.L.B., G.M.Y., A.J.Y.), Pharmacology (J.W.R., A.J.Y.), and Pharmacology and Toxicology (T.L.A., S.L., J.W.R.), University of Arizona College of Pharmacy, Tucson, Arizona; and Programs in Pharmacology and Toxicology (G.M.Y., J.W.R., A.J.Y.) and Neuroscience (D.B., J.W.R., A.J.Y.), University of Arizona, Tucson, Arizona

Received July 6, 1999; accepted December 11, 1999

This paper is available online at http://www.molpharm.org

ABSTRACT

Aquaporin-1 (AQP1) is a member of the membrane intrinsic protein (MIP) gene family and is known to provide pathways for water flux across cell membranes. We show here that cloned human AQP1 not only mediates water flux but also serves as a cGMP-gated ion channel. Two-electrode voltage-clamp analyses showed consistent activation of an ionic conductance in wild-type AQP1-expressing oocytes after the direct injection of cGMP (50 nl of 100 mM). Current activation was not observed in control (water-injected) oocytes or in AQP5-expressing oocytes with osmotic water permeabilities equivalent to those seen with AQP1. Patch-clamp recordings revealed large conductance channels (150 pS in K^+ saline) in excised patches from AQP1-expressing oocytes after the application of cGMP to the internal side. Amino acid sequence alignments between AQP1 and sensory cyclic-nucleotide-gated channels showed similarities between the cyclic-nucleotide-gated binding domain and the AQP1 carboxyl terminus that were not present in AQP5. Competitive radioligand-binding assays with [^{3}H]cGMP demonstrated specific binding (K_D = 0.2 μM) in AQP1-expressing Sf9 cells but not in controls. These results indicate that AQP1 channels have the capacity to participate in ionic signaling after the activation of cGMP second-messenger pathways.

Aquaporin-1 (AQP1) channels provide high transmembrane water movement for a specialized subset of mammalian tissues, including red blood cells, kidney (proximal tubule and descending Henle's loop), eye (ciliary epithelia, trabecular meshwork, and canals of Schlemm), brain (choroid plexus), lung (peribronchial vasculature), and other tissues, including lymph vessels and muscle (King and Agre, 1996). Aquaporins are believed to exist as homotetramers, with individual subunits consisting of six predicted transmembrane domains and internal amino and carboxyl termini (Agre et al., 1993). This subunit structural motif also is a hallmark of the ion channel gene family that includes potassium channels and cyclic-nucleotide-gated (CNG) channels from retinal and olfactory cells (Jan and Jan, 1992).

Several members of the membrane intrinsic protein (MIP) family of channels have been shown to carry ionic currents. Reconstitution of MIP into lipid bilayers yielded large-conductance ion channels with single-channel events showing unitary conductances of 180 and 380 pS, long open times, and symmetrical activation over a range of voltages in 100 mM KCl saline (Ehring et al., 1990). Reconstitution of another MIP family member, Nodulin26, into lipid bilayers also yielded single channels with high unitary conductances and several subconductance states (Weaver et al., 1994). Reconstitution of AQP1 into lipid bilayers yielded large-conductance ion channels that were interpreted as artifacts of the lipid bilayer method (Mulders et al., 1995). Earlier voltage-clamp studies of AQP1 expressed in oocytes provided no evidence of ionic permeability (Preston et al., 1992; Raina et al., 1995); however, we found that stimulation with forskolin, 8-bromo-cAMP (8-Br-cAMP), or the catalytic subunit of protein kinase A (PKA) activated a nonselective cation conductance in AQP1-expressing oocytes that was not seen in control oocytes (Yool et al., 1996). Based on reversal potentials measured in ion substitution studies, the cationic permeability of the activated channel was determined to be $K^+ = Cs^+ \geq Na^+ \gg$ tetraethylammonium; conversely, isosmotic substitution of chloride with gluconate, aspartate, or acetate had no appreciable effect on reversal potential, indicating that

This work was supported by American Heart Association Grants 96007629 and 9951130Z, National Institutes of Health Grant R01-EY11291-02, and the Arizona Kidney Foundation.

ABBREVIATIONS: AQP1, aquaporin-1; Sf9, *Spodoptera frugiperda*; AQP5, aquaporin-5; CNG, cyclic nucleotide gated; MIP, membrane intrinsic protein; 8-Br-cAMP, 8-bromo-cAMP; PKA, protein kinase A; H7, 1-(5-isoquinolinesulfonyl)-2-methylpiperazine dihydrochloride; RP-8-Br-PET-cGMPS, β-phenyl-1,N^2-etheno-8-bromoguanosine-3′,5′-cyclic monophosphoro-thioate Rp-isomer; 8-pCPT-cGMP, 8-(4-chlorophenylthio)-guanosine-3′,5′-cyclic monophosphate; SP-8-Br-PET-cGMPS, β-phenyl-1,N^2-ethano-8-bromoguanosine-3′,5′-cyclic monophosphoro-thioate Sp-isomer; SSC, standard saline citrate.

anionic permeability was negligible (Yool et al., 1996). The ionic conductance response was inhibited by pretreatment of oocytes with the protein kinase inhibitor 1-(5-isoquinolinesulfonyl)-2-methylpiperazine dihydrochloride (H7), suggesting involvement of a kinase. The conductance also was blocked by $HgCl_2$, a known inhibitor of AQP1 water permeability. We concluded that ionic permeability in AQP1-expressing oocytes required intracellular signaling, whereas water permeability was a feature of both the stimulated and unstimulated states. Recently, pH-sensitive ion channel function has been described for AQP6 expressed in oocytes (Yasui et al., 1999).

Our conclusion that AQP1 is a regulated ion channel remains controversial (data not shown; Yasui et al., 1999). Other investigators have either reproduced aspects of our findings (Fischbarg et al., 1997; Patil et al., 1997b) or found that they could not generate the response to forskolin in AQP1-expressing oocytes (Agre et al., 1997; Deen et al., 1997). Patil et al. (1997a) confirmed that significant increases in water flux were measured for AQP1-expressing oocytes after direct injection of 8-Br-cAMP or stimulation with arginine vasopressin, thought to act via PKA. We confirmed inconsistencies in the ionic response to forskolin but noted that the direct injection of the catalytic subunit of PKA continued to be a reliable inducer of the conductance response.

We speculated that the pathway involved in AQP1 activation might be subject to variation in forskolin sensitivity among different preparations of oocytes, as has been seen in other studies (Smith et al., 1987; Miledi and Woodward, 1989). In searching for more direct regulatory pathways, we noted the presence of sequence similarities between the carboxyl tail domains of AQP1 and CNG channels and tested the role of direct cyclic nucleotide binding in the activation of the ionic conductance. We show here that cGMP activates an ionic current in AQP1-expressing oocytes as measured by both two-electrode voltage-clamp and patch-clamp recordings but does not activate an ionic conductance response in AQP5-expressing oocytes, in oocytes injected with a nonfunctional mutant AQP1, or in control oocytes. The inductive effect of cGMP on AQP1 channels is not blocked by H7, suggesting that current activation results from the direct binding of cGMP rather than the activation of a kinase. This idea is further supported by radioligand binding assays with [^{3}H]cGMP that showed specific binding in membranes prepared from AQP1-expressing Sf9 cells but not in membranes from control Sf9 cells. These data support our hypothesis that AQP1 has the capacity to form ion-conducting channels that can be activated directly by cGMP binding or indirectly through the activation of a kinase.

Materials and Methods

Oocyte Preparation and Injection. Oocytes at stages V and VI were harvested from female *Xenopus laevis* and prepared by incubation for 1 to 3 h in collagenase (1.5 mg/ml Type 1, Worthington Biochemicals, Freehold, NJ) in the presence of trypsin inhibitor (0.5 mg/ml Type III-0; Sigma Chemical Co., St. Louis, MO). Oocytes were injected the day after isolation with either 50 nl of water (control oocytes); or 50 nl of water containing AQP1 or AQP5 cRNA. Oocytes were maintained for 2 to 7 days at 18°C in ND96 culture medium (96 mM NaCl, 2 mM KCl, 1.8 mM $CaCl_2$, 2.5 mM Na-pyruvate, 5 mM HEPES, pH 7.6) to allow the expression of aquaporin channels. Successful expression was checked by placing an oocyte in distilled water; aquaporin-expressing oocytes swelled quickly and burst, whereas control and noninjected oocytes remained virtually unchanged in appearance for up to 10 min in distilled water. The injection of 1 ng of AQP1 or AQP5 cRNA per oocyte provided moderate levels of protein expression useful for two-electrode voltage-clamp and swelling assays; 20 ng of AQP1 cRNA per oocyte gave correspondingly higher expression levels that were useful for patch-clamp recordings.

Wild-Type and Mutant Constructs. Wild-type human AQP1 (CHIP28) and rat AQP5 cDNAs were provided by Dr. Peter Agre. AQP5 was subcloned into the same 5′,3′ *Xenopus* β-globin UTR plasmid vector as used for AQP1. Capped cRNA transcripts were synthesized in vitro with T3 RNA polymerase enzyme, using *Bam*HI-linearized cDNA as a template. The RNA concentration was determined by UV absorbance spectrophotometry to standardize the amounts of RNA injected into the oocytes. A nonfunctional mutant AQP1 Y186N (Brooks et al., 2000) was made by site-directed mutagenesis and was found to confer no permeability to water or ionic conductance, with or without cGMP treatment. For site-directed mutagenesis of AQP1, the segment between restriction enzyme sites *Eco*RI and *Not*I in the AQP1 expression vector (Preston et al., 1992) was replaced with a cassette containing the point mutation, previously generated by a two-step polymerase chain reaction. The mutation of Tyr186 to asparagine (Y186N) was made with sense primer 5′-GGCTATTGACAACACTGGCTGTGGG-3′ and antisense primer 5′-TACCTAGCATGAACAGATTGGTAATACGACTCACTATA-3′. The desired mutation in the correct reading frame was confirmed by DNA sequencing.

Swelling. Osmotic swelling was analyzed from volume changes recorded by video camera with images captured every 15 s (IPLab Spectrum software). Water permeability assays at 22°C were initiated with the transfer of aquaporin-expressing or control oocytes at time zero from 200 mOsM control ND96 saline into 100 mOsM ND96 diluted with distilled water, and images were collected through 6 min or until the oocytes ruptured. Data were analyzed as the proportional change in volume with time and standardized to the initial volume at time zero.

Electrophysiology. For two-electrode voltage-clamp, borosilicate electrodes were filled with 3 M KCl (1–3 MΩ). Recordings were done in Na^+ bath saline containing 100 mM NaCl, 2 mM KCl, 4.5 mM $MgCl_2$, and 5 mM HEPES, pH 7.3. Two-electrode recording pipettes were used conventionally to control voltage and deliver current. A third sharp pipette, held in a separate micromanipulator and connected by a mineral oil-filled tube to a Drummond micropipette device, was used to deliver 40 to 50 nl of freshly loaded 8-Br-cGMP solution (100 mM) or an equivalent volume of saline (sham injection) into the voltage-clamped oocyte during the recording. Aliquots of 8-Br-cGMP were loaded into the injection pipette immediately before each injection event to minimize partition of the agonist into the mineral oil. Conductance responses were measured before, during, and after injection of 8-Br-cGMP or saline vehicle into the oocyte. Sham injections confirmed that the on-line injection process itself induced no conductance artifacts. Borosilicate pipettes (0.3–1.5 MΩ) were used for patch recordings. The K^+ saline in the pipette consisted of 40 mM KCl, 60 mM K gluconate, 5 mM $MgCl_2$, and 10 mM HEPES, pH 7.3. High K^+ bath saline faced the internal (formerly cytoplasmic) side of the excised inside-out patch, as indicated. In preparation for recording by patch-clamp, vitelline membranes of the oocytes were stripped manually after brief treatment of the oocyte with stripping medium (200 mM *N*-methylglucamine buffered with aspartic acid, 20 mM KCl, 10 mM EGTA, 1 mM $MgCl_2$, 10 mM HEPES, pH 7.3) and oocytes were rinsed in K^+ bath saline. Patches were excised from the oocyte in the inside-out configuration; then, cGMP or cAMP (chemically unmodified) was applied in the K^+ bath saline. Recordings were made with a GeneClamp amplifier and pClamp software (Axon Instruments, Foster City, CA). Data were filtered at 2 kHz, digitized at 10 kHz, and stored to hard disk for

off-line analysis. cGMP, 8-Br-cGMP, and cAMP were purchased from Sigma Chemical Co. and Research Biochemicals Inc. (Natick, MA). From BioLog, Life Science Institute (La Jolla, CA), we obtained β-phenyl-1,N^2-etheno-8-bromoguanosine-3′,5′-cyclic monophosphoro-thioate Rp-isomer (Rp-8-Br-PET-cGMPS), an inhibitor of cGMP-dependent protein kinase and of retinal cGMP-gated ion channels; β-phenyl-1,N^2-ethano-8-bromoguanosine-3′,5′-cyclic monophosphoro-thioate Sp-isomer (Sp-8-Br-PET-cGMPS), an inhibitor of retinal cGMP-gated channels but an activator of cGMP-dependent protein kinase; and 8-(4-chlorophenylthio)-guanosine-3′,5′-cyclic monophosphate (8-pCPT-cGMP), an activator of cGMP-gated ion channels and of cGMP-dependent protein kinase.

Transfection of Sf9 Cells with AQP1 for [^{3}H]cGMP Binding Assay. Sf9 cells were infected with recombinant baculovirus carrying the human AQP1 gene to yield high levels of AQP1 protein production; control Sf9 cells were infected with recombinant baculovirus lacking the AQP1 sequence. For the transfection procedure, the Sf9 cells were equilibrated in Sf900 medium (Life Technologies, Grand Island, NY) before infection; then, 4×10^5 cells/ml were suspended in 70 ml of Sf900 media and infected with virus (1 PFU/cell) for 2 days at 29°C. Viability was examined on days 3 to 7 using a trypan blue exclusion assay, and Sf900 medium was added to maintain the cells at a concentration of 5 to 10×10^5 cells/ml. Cells were harvested when the infection level approached 90 to 100%; at this time, 75 ml each of the cell suspensions was collected and centrifuged (3500 rpm, 10 min, 4°C). The pellets were washed twice in PBS and once in buffer containing HEPES (5 mM, pH 7.4), dextrose (5.6 mM), and NaCl (137 mM) and then resuspended in 20 ml of 5 mM Tris buffer containing $MgCl_2$ (5 mM) and EGTA (1 mM, pH 7.5) and frozen at −80°C. Suspensions were thawed on ice in aliquots of 10 ml with protease inhibitors, homogenized cold, and centrifuged (500*g*, 5 min, 4°C). After examination under a microscope for the removal of nuclei, the supernatants were diluted to 40 ml using Tris buffer and centrifuged using a SW-27 rotor (100,000*g*, 30 min, 4°C). The pellets were resuspended in Tris buffer, and the total protein concentrations were determined. The concentrations of Sf9 cell total protein in the samples were standardized to 1 mg/ml by the addition of an appropriate volume of buffer (10 mM HEPES, pH 7.4, 10 mM $MgCl_2$, 1 mM EGTA, 1 mg/ml 3-isobutyl-1-methylxanthine). Serial dilutions of cold cGMP (6.4×10^{-9} to 6.4×10^{-3}) were prepared in aliquots of 115 μl/tube; an additional tube contained an equal volume of buffer without cGMP. Sf9 membrane protein preparations (185 μl, 1 mg/ml) were added to each dilution of cold cGMP, vortexed, and incubated on ice for 30 min. Then, 2 μCi of [^{3}H]cGMP (Amersham; specific activity, 10.7 Ci/mmol) was added to each tube. Tubes were vortexed and then rotated for 6 h at 4°C. Finally, 145 μl of each sample was added to 1.5-ml tubes containing 290 μl of a mixture (3:2, v/v) of dibutyl phthalate (Sigma Chemical Co.) and dioctyl phthalate (Aldrich), and tubes were centrifuged at 12,000 rpm at 25°C. Radioactivity in the pellets was determined by liquid scintillation counting.

Immunofluorescence Microscopy in Sf9 Cells. Sf9 cells expressing AQP1 and control Sf9 cells were grown on glass coverslips; the medium was removed, and the cells were washed with PBS. Coverslips were placed in 4% paraformaldehyde in PBS for 10 min at room temperature and washed once with PBS. Nonspecific binding was blocked with 2% BSA for 1 h at 4°C. The slides were rinsed briefly with standard saline citrate (SSC) buffer and then permeabilized in SSC buffer containing 0.1% Triton X-100 for 1 h at 4°C. After an overnight incubation with primary antibody (0.5–1.0 mg/ml, 4°C), the slides were washed with SSC buffer and incubated for 1 h at room temperature with secondary antibody (donkey anti-rabbit antibodies tagged with fluorescein isothiocyanate; Sigma Chemical Co.) at a dilution of 1:1000. Sf9 cells were viewed with a compound fluorescence light microscope (BH-5; Olympus) using an excitation filter of 495 nm. Rabbit polyclonal antibodies, generated against unique carboxyl-terminal domains of AQP1 and AQP5 (as glutathione-*S*-transferase-linked fusion peptides), were specific in labeling only the corresponding aquaporin proteins in transfected fixed and permeabilized COS cells. Labeling was blocked effectively by preincubation of antibody with the appropriate fusion peptide. Neither antibody cross-reacted with other classes of aquaporins expressed in COS cells (AQP1: Stamer et al., 1995; AQP5: G.M.Y., J.W.R., and A.J.Y., unpublished data).

Results

A previously unrecognized amino acid sequence similarity between the carboxyl-terminal domains of AQP1 and CNG channels (Fig. 1) suggested the presence of a cyclic-nucleotide-binding domain in AQP1. In sensory CNG channels, the carboxyl terminus has been shown by mutagenesis studies to be involved in cyclic nucleotide binding (Goulding et al., 1994; Varnum et al., 1995). In contrast to AQP1, a CNG-like sequence pattern in the carboxyl tail is not as apparent for the other members of the MIP family such as AQP5, although some similarities exist. This similarity between amino acid sequences for AQP1 and CNG channels suggested the presence of a potential binding site that might be important for channel activation.

Figure 2 shows single-channel activity recorded from an excised inside-out patch from an AQP1-expressing oocyte. The large conductance channel was activated after bath application of ~0.1 mM cGMP (4 μl of 10 mM into 400 μl of K^+ bath saline) to the internal (formerly cytoplasmic) face of the patch. In the excised-patch configuration, membrane proteins are removed from the influence of intracellular signaling processes. Figure 2A shows cGMP-induced channel activity in superimposed traces (eight each), as seen without leak or capacitance subtraction. Figure 2, B and C, shows blank-

Gene	AA#	Carboxy tail sequence
hAQP1	229-269	FILAPRSSDLTDRVKVWTSGQVEEYDLDA....DDINSRVEMKPK
rOlf(1)	541-597	NIRSLGYSDLFCLSKDDLMEAVTEYP.DAKKVLEERGREILMKEGLLDENEVAASMEV+
rOlf(2)	433-489	NIKSLGYSDLFCLSKEDLREVLSEYP.QAQAVMEEKGREILLKMNKLDVNAEAAEIAL+
fOlf	532-588	NIRSIGYSDLFCLSKDDLMEAVAEYP.DAQKVLEERGREILRKQGLLDESVAAGGLGV+
bRet	562-618	NIKSIGYSDLFCLSKDDLMEALTEYP.DAKGMLEEKGKQILMKDGLLDINIANAGSDP+
rAQP5	228-265	SSLS..LHDRVAVVK.....GTYEPEEDWEDHREERKKTIELTAH

Fig. 1. Alignment of the carboxyl-terminal domains of AQP1, AQP5, and cyclic nucleotide-gated channels. Amino acid numbers are for the segment shown. Conserved residues are marked in bold; dots indicate gaps introduced for alignment; similar residues are underlined; and + indicates additional sequence not shown. Sources of sequence data are hAQP1 (human aquaporin-1; Preston and Agre, 1991), rOlf(1) (rat olfactory CNG; Dhallan et al., 1990), rOlf(2) (rat olfactory CNG; Bradley et al., 1994), fOlf (catfish olfactory CNG; Goulding et al., 1992), bRet (bovine retinal CNG; Kaupp et al., 1989), and rAQP5 (rat aquaporin-5; Raina et al., 1995).

subtracted traces for consecutive sweeps recorded in the continuous presence of cGMP after a single bath application of agonist, with voltage stepped to +30 mV or −60 mV from a holding potential of −20 mV. The channel activity during the prolonged response alternated between modes with long openings that were sustained for the full voltage step, and traces with either no activity, or flickery openings reminiscent of subconductance states that have been described for CNG channels (Ruiz and Karpen, 1999) and other channels.

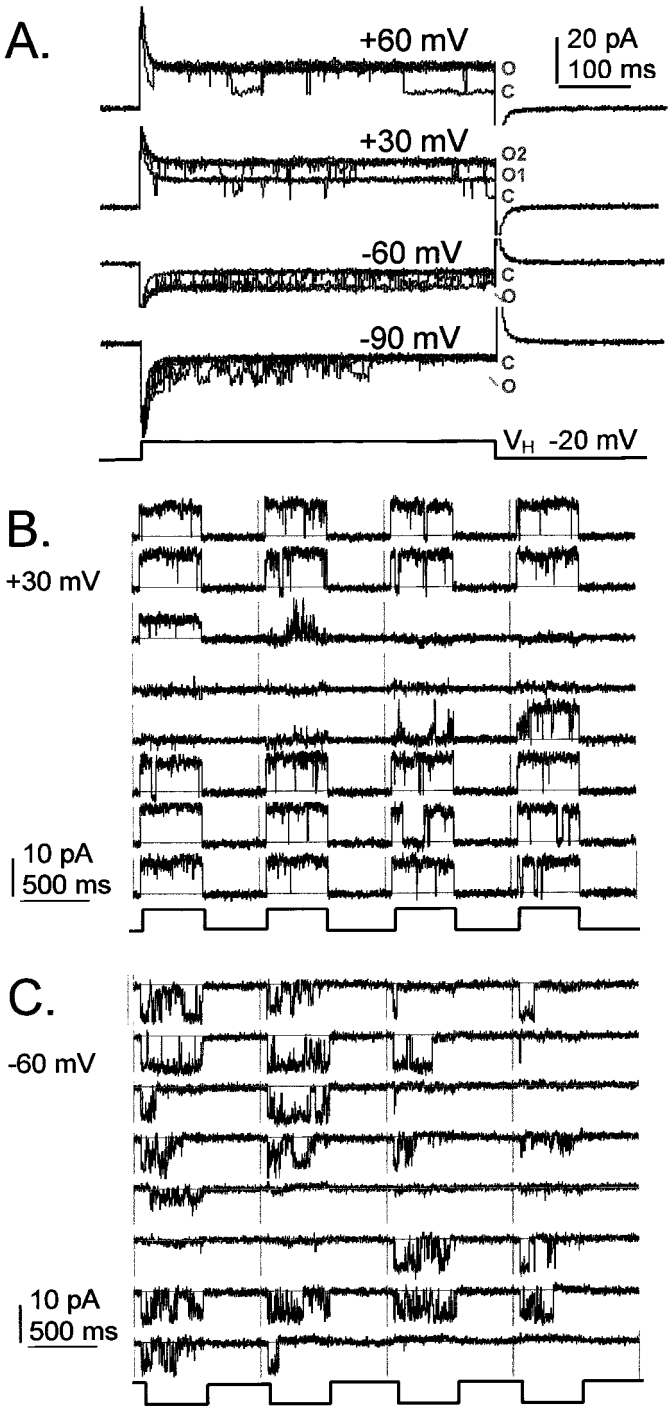

Fig. 2. Ion channel activated by cGMP in an inside-out patch from an AQP1-expressing oocyte. Channel events were activated by bath application of ~0.1 mM cGMP to the internal face of the patch. A, eight superimposed traces for each voltage step are shown without leak or capacitance subtraction (O, open; C, closed). Blank-subtracted recordings show consecutive traces (separated by vertical lines) for a repeated step-voltage protocol to +30 mV (B) or −60 mV (C) from a holding potential of −20 mV. Leak and capacitance were subtracted using an averaged set of blank traces from the same patch.

Figure 3 shows data compiled for a single-channel inside-out patch from an AQP1-expressing oocyte, activated by bath application of ~0.1 mM cGMP. Single-channel conductance was calculated from the linear current-voltage relationship (Fig. 3A). Channel current amplitudes (mean ± S.D.) at each voltage were determined from gaussian fits of amplitude histograms for fully open channels and plotted as a function of membrane potential (pipette command potential multiplied by −1). The unitary conductance for the cGMP-activated channel in excised patches was 145 ± 5 pS (mean ± S.D.; n = 4 patches). Application of cGMP was successful in activating the large conductance channels in 7 of 12 excised patches from AQP1-expressing oocytes injected with 20 ng of cRNA and from 1 of 8 patches from AQP1-expressing oocytes injected with only 1 ng of cRNA. Responses typically were sustained in the continued presence of cGMP for several minutes. However, in two patches from AQP1-expressing oocytes, cGMP application caused only a transient activation of similarly large amplitude channels for which unitary conductances were not calculated. In contrast, the bath application of ~1 mM cAMP was not found to be effective in activating channels in 3 of 3 inside-out patches, as confirmed in 2 patches for which subsequent application of cGMP did activate channels. In 1 of 2 cell-attached patches from AQP1-expressing oocytes, bath-applied 8-Br-cAMP was successful in activating the large conductance channel, but channel activity was not sustained when the patch was pulled into the inside-out configuration. Control oocytes did not express high conductance channels, with or without the application of cGMP (n = 7 patches). The apparent lack of a direct effect of cAMP is consistent with previous data showing that the activating effect of cAMP occurs indirectly through a pathway that is sensitive to H7 (Yool et al., 1996), in contrast to the effects of cGMP, which are insensitive to H7 (see later). The possible partial agonist or antagonist effects of higher concentrations of cAMP remain to be determined.

Open probability (Fig. 3B) was analyzed by integrating a constant area (480 ms) under each current trace during a voltage step; these values were adjusted by subtracting the averaged integrated area for blank traces and were standardized to the maximum value of integrated area determined for a continuously open channel (set as P_o = 1.0). Open probability values were plotted as frequency histograms for data collected from the same single-channel patch over a range of voltages, for 64 to 130 sweeps per voltage. At positive potentials (+60, +30 mV), the fully open channel mode (0.9–1.0) was common. At −60 mV, the bimodal pattern of channel activity showed comparable frequencies of inactive (0–0.1) and fully active (0.9–1.0) channel modes. At −90 mV, many traces showed transient channel activity, and traces with channels remaining fully open through the duration of the voltage step were rare. Comparable patterns of voltage-sensitive activity were observed in the other cGMP-stimulated patches from AQP1-expressing oocytes.

The time course of the single-channel open probability response to a repeated application of cGMP is shown in Fig. 3C (for the same patch as shown in Fig. 3, A and B). Open probabilities (calculated as described for Fig. 3B) were plot-

ted as a function of time for consecutive traces. The excised inside-out patch showed no AQP1 channel activity before the application of cGMP. After a latency of ~2 min after the addition of 4 μl of cGMP (10 mM) to the bath, channel open probability increased and remained elevated for ~5 min. The long latency period reflects an unusually slow process of binding and activation of the channel; the rate-limiting step in the activation process remains to be identified. During the response, the channel did not remain in the fully open mode but showed excursions to lower probability states. A brief interlude at −120 mV (at 190–230 s) transiently suppressed channel activity but did not prevent resumption of the response with the subsequent return to a depolarized voltage-step protocol. A second application of cGMP evoked a comparable response after a similar latency. Figure 3, D and E, shows recordings of consecutive traces of channel activity at the onset of the channel response to cGMP at times a and b, respectively (as indicated in Fig. 3C). The traces illustrate the transition from no activity, through a period of flickery channel activity, to the activation of the fully open mode.

Figure 4 shows ensemble averages of cGMP-induced channel activity in an excised patch containing at least three

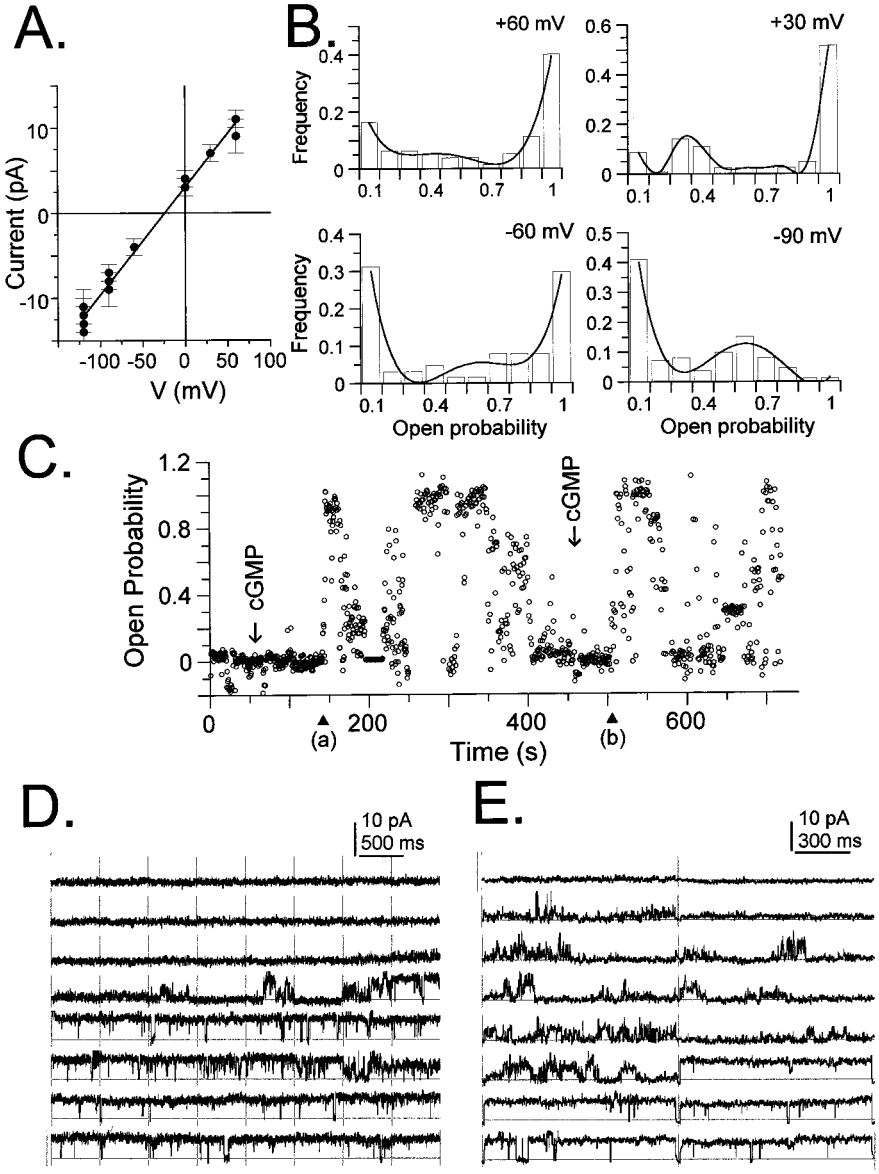

Fig. 3. AQP1 channel open probability and conductance properties in an inside-out patch containing a single channel, after application of ~0.1 mM cGMP. A, the unitary current-voltage relationship shows a linear relationship. Data for mean ± S.D. unitary current amplitude were calculated from the gaussian fits of amplitude histograms using pClamp software. Multiple data points per voltage reflect analyses made at different times during the prolonged response to cGMP. B, open channel probability was calculated from the integrated area under blank-subtracted current traces (480 ms) during voltage steps to +60, 30, −60, or −90 mV from a holding potential of −20 mV and was standardized to the maximal value for the integrated current determined for the fully open channel state. Frequency histograms show the relative occurrence of channel open probabilities. See text for details. C, open channel probabilities calculated for the same channel as illustrated in A and B, plotted for consecutive traces as a function of time during the recording. Arrows show the times of application of cGMP to the bath (4 μl of 10 mM cGMP in K^+ saline, into 400-μl bath). Markers (a) and (b) indicate times of onset of channel activity and correspond to the traces illustrated in D and E, respectively. D and E, consecutive traces delimited by vertical lines show channel transitions from inactivity through a flickery phase to the fully open channel mode in response to cGMP. Nonsymmetrical bath saline contained 60 mM KCl and 90 mM K^+ gluconate.

channels, from an AQP1-expressing oocyte. Ensemble averages (Fig. 4A) were generated from 32 consecutive blank-subtracted sweeps at each voltage. Examples of individual traces that were used to generate the ensemble averages are shown in Fig. 4B. Averaged currents at depolarized potentials showed profiles similar to those seen for the macroscopic currents recorded by two-electrode voltage-clamp. However, averaged currents at hyperpolarized potentials showed a more substantial decay component than was observed in two-electrode voltage-clamp recordings (see *Discussion*).

Figure 5 shows two-electrode voltage-clamp analysis of ionic current activation by 8-Br-cGMP in an AQP1-expressing oocyte (Fig. 5A). The AQP1-expressing oocyte was sham-injected with saline vehicle at 4 min. Penetration of the oocyte with the injection pipette caused a brief current artifact, but the sham injection did not stimulate an ionic conductance. The subsequent application of 8-Br-cGMP in the bath (final concentration ~0.7 mM) evoked a minimal response. Increasing the concentration of 8-Br-cGMP to ~7 mM evoked an ion conductance response after a latency of ~10 min. This higher concentration requirement and slower response time differ from the results of the excised-patch study and are likely to reflect a limiting rate of diffusion of the agonist across the oocyte membrane. In support of this idea, we have found that the direct injection of 8-Br-cGMP during two-electrode voltage-clamp recordings is more effective and rapid for inducing the ionic conductance response than is bath-applied agonist (see later). The relatively low permeability of oocyte membranes even to "membrane-permeant" cGMP derivatives has been noted previously in other laboratories (W. Zagotta, personal communication). Figure 5, B and C, shows the net 8-Br-cGMP-activated current plotted as a function of voltage, and the corresponding net currents, for the same oocyte as shown in Fig. 5A. Net current was determined by subtracting the initial current (at time zero) from the maximal 8-Br-cGMP-activated current. An alternative method for activating the channels is to preincubate the oocytes in 10 mM 8pCPT-cGMP for 15 min before electrophysiological recording; the current then develops during the depolarization protocol in the continued presence of 8pCPT-cGMP in the bath saline, following a time course of activation similar to that seen with direct injection studies (see later, results for Fig. 9).

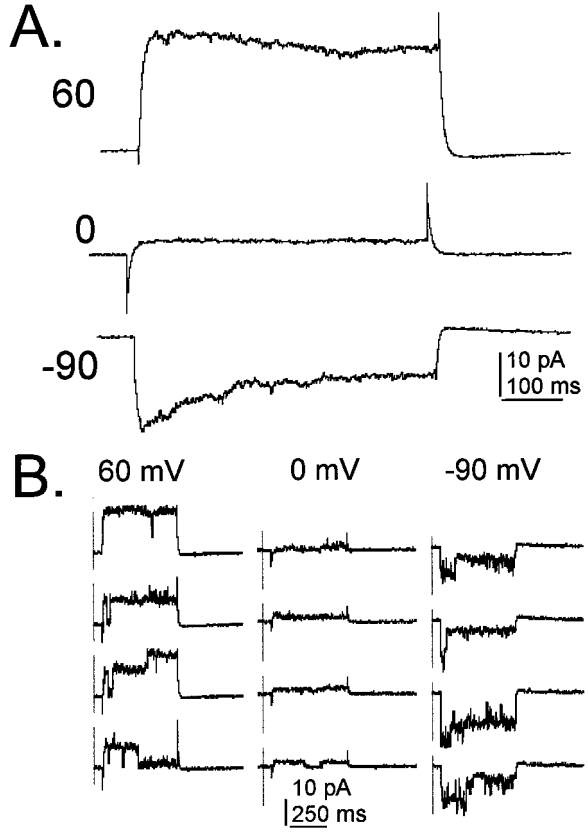

Fig. 4. Ensemble averaged currents from an inside-out patch containing multiple AQP1 channels, illustrating properties of the cGMP-activated ionic conductance response. A, an inside-out patch from an AQP1-expressing oocyte containing at least three AQP1 channels was used to generate an ensemble average from 32 consecutive traces at each voltage. B, examples of individual traces used in the generation of the ensemble average.

Figure 6A summarizes the net conductance responses of AQP1-expressing and control oocytes to injection of 8-Br-cGMP or to sham injections in two-electrode voltage-clamp recordings. Net conductance (μS) was determined from a linear fit of the current-voltage relationship from +60 to −80 mV (holding potential −40 mV) for the net current response at 10 min after injection. Repeated steps to +40 mV were applied throughout the recordings before, during, and after injections at 5-s intervals to monitor the development of the ionic conductance response for all treatment conditions, except where otherwise specified. Activation of the AQP1 ionic conductance was dependent on the injection of 8-Br-cGMP, was not stimulated by sham injections, and was insensitive to the kinase antagonist H7 (10 μM). The rate of activation of the ionic conductance response after 8-Br-cGMP injection was slower in AQP1 oocytes that were held constantly at −40 mV, compared with AQP1 oocytes subjected to the routine application of repetitive +40-mV steps.

For AQP1 oocytes held at −40 mV, only a small increase in net conductance was induced by the 8-Br-cGMP injection alone. However, the subsequent application of the +40-mV step protocol for an additional 10 min further stimulated the ionic conductance response to levels comparable to those seen for AQP1 oocytes that had been simultaneously stimulated with 8-Br-cGMP and +40-mV steps (Fig. 6B). Traces of current responses to a set of voltage steps (+60 to −80 mV, from a holding potential of −40 mV) in Fig. 6C illustrate the net conductances in oocytes that were stimulated simultaneously with 8-Br-cGMP and depolarization, compared with oocytes that were held at −40 mV for 10 min after the injection of 8-Br-cGMP and then subjected to the depolarization step protocol (sequential stimulation). These data suggested that cGMP agonist was required for channel activation but that the rate of development of the macroscopic current response was enhanced by depolarization, suggesting that by favoring the open state of the channel, positive voltages increased the proportion of channel residence time in a higher-affinity state.

After penetration with the recording electrodes, AQP1-expressing oocytes sometimes showed a spontaneous activation of the ionic conductance that varied in magnitude between batches of oocytes, that was blocked by H7, and that probably reflected basal levels of activity of PKA (Fig. 6A, AQP1, sham-injected versus sham-injected with H7). The similar levels of the maximal responses of AQP1-expressing

oocytes to 8-Br-cGMP, with or without preincubation in H7, suggested that the spontaneous and evoked currents were likely to be mediated by the same population of channels. Control oocytes, not expressing AQP1, showed no significant response to injection of 8-Br-cGMP, with either simultaneous or sequential applications of the +40-mV step protocol (Fig. 6A, control). In some control oocytes, at the end of the experiment an excessive volume (~150–200 nl) of 100 mM 8-Br-cGMP was injected until the oocytes were visibly swelled, yet no currents were evoked (data not shown). This indicates that the ionic conductance activated by injection was not due to a stretch-activated current.

As a control for possible nonspecific effects of the overexpression of AQP1 protein in oocyte membranes, we evaluated responses for a mutant AQP1 in which Tyr186 was mutated to asparagine (Y186N; Fig. 6A). This construct was one of a series of loop E (pore region) mutations that were generated in our laboratory to determine the molecular site of action of a novel pharmacological blocker of AQP1-mediated water permeability (Brooks et al., 2000). The mutant Y186N protein was found to be expressed abundantly in plasma membrane (immunocytochemical data not shown) but was nonfunctional with respect to both ionic permeability (Fig. 6A) and water permeability (data not shown). The expression of nonpermeant AQP1 Y186N yielded no spontaneously activating current responses; Y186N-expressing oocytes were indistinguishable from control oocytes. The lack of a conductance response with AQP1 Y186N suggests that the physical translocation of AQP1 protein to the oocyte membrane does not recruit native channels.

Figure 7 shows the results of [^{3}H]cGMP-binding assays performed with membranes from the Sf9 cells infected with baculovirus encoding AQP1 or infected with baculovirus alone. In both cases, unlabeled cGMP competed for the binding of [^{3}H]cGMP; however, in the membranes expressing AQP1, the dose-response relationship was shifted two orders of magnitude to the left and was consistent with the formation of a new population of cGMP-binding sites with a mean K_D value of 0.2 μM. Immunofluorescence microscopy of Sf9 cells infected with recombinant baculovirus encoding AQP1 showed very strong immunoreactivity with antibody to AQP1 (Fig. 7A) that was absent in Sf9 cells infected with the virus alone (Fig. 7B).

Our alignment of the carboxyl-terminal amino acid sequences (see Fig. 1) suggested that AQP1 showed a degree of homology with the CNG-binding domain that was not as apparent for other members of the aquaporin gene family. This observation was tested by evaluating the response of AQP5-expressing oocytes to the injection of 8-Br-cGMP (Fig. 8). The injection of 8-Br-cGMP into AQP5-expressing oocytes did not induce any ionic conductance response, whereas the comparable treatment of AQP1-expressing oocytes was effective (Fig. 8A). However, the AQP5-expressing oocytes did show high osmotic water permeability equivalent to that of AQP1, indicating comparable levels of channel expression for AQP1 and AQP5 (Fig. 8B). These results demonstrated that the ionic conductance response of AQP1-expressing oocytes cannot be attributed indirectly to the increased membrane water permeability in oocytes as a result of aquaporin expression. Spontaneous activation of ionic current in AQP1-expressing oocytes was evident in the increase in current amplitude seen before injection of 8-Br-cGMP and was blocked by H7 (Fig. 8C). In contrast, AQP5-expressing oocytes produced no spontaneously activating current and no 8-Br-cGMP-induced response, showing that both the spontaneous activation and the induced response are specifically dependent on the expression of AQP1 channels. The net conductance response to 8-Br-cGMP in AQP1-expressing oo-

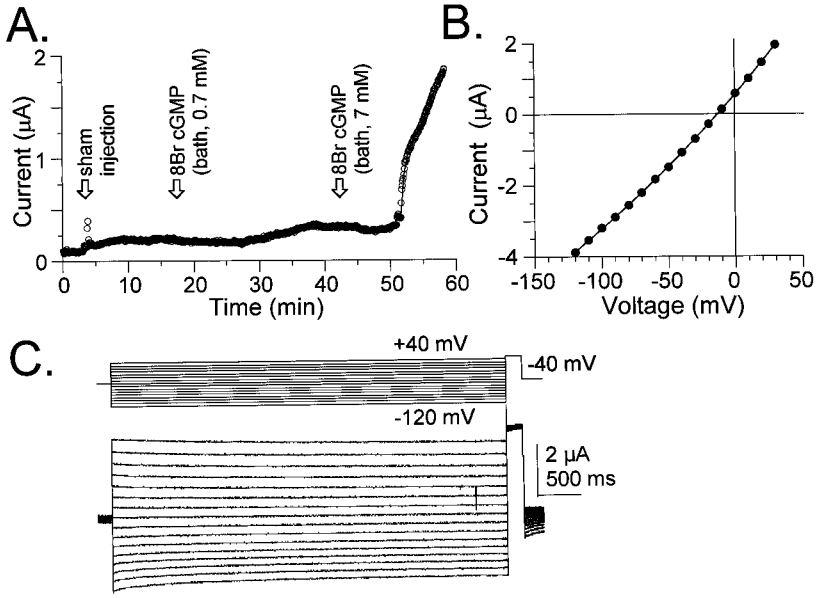

Fig. 5. Two-electrode voltage-clamp recording of the ionic current activated by 8-Br-cGMP in an AQP1-expressing oocyte. A, on-line injection of 50 nl of saline into an AQP1-expressing oocyte (sham-injection; first arrow) during a recording elicited no ionic conductance response. Data points show the current amplitude measured at +40 mV plotted as a function of time during the recording using a depolarization step protocol (step to +40 mV for 0.8 s, once every 5 s, from a holding potential of −40 mV). Subsequent bath applications of 8-Br-cGMP confirmed the presence of cGMP-sensitive channels and showed a dose-dependent response. B, plot of the current-voltage relationship for peak current for the traces shown in C. C, current-voltage response of the net cGMP current after achieving the maximal response (after 60-min time point in A). The voltage protocol used steps from −120 mV to +30 mV in increments of +10 mV, followed by a brief step to +40 mV, from a holding potential of −40 mV, to assess the properties of the activated conductance over a range of voltages.

cytes reached comparable levels, regardless of whether the response was preceded by a period of spontaneous activation (AQP1 responses with and without H7; Fig. 8D). In contrast, the net conductance after 8-Br-cGMP injection of AQP5-expressing oocytes was indistinguishable from that of control oocytes.

Figure 9 shows that cGMP-mediated activation of the ionic conductance in AQP1-expressing oocytes can be mimicked by a known agonist of CNG channels (8pCPT-cGMP) and blocked by CNG channel antagonists (Sp-8-Br-PET-cGMPS and Rp-8-Br-PET-cGMPS). These data suggest that the carboxyl tail sequence homology between AQP1 and CNG channels correlates with similarities in pharmacological binding site properties. The effects of the pharmacological agents also argue against a contribution of cGMP-dependent protein kinase to the activation of the current. Specifically, Sp-8-Br-PET-cGMPS is an inhibitor of retinal cGMP-gated channels but an activator of cGMP-dependent protein kinase. Its ability to inhibit the ionic conductance response to cGMP agonist in AQP1-expressing oocytes indicates that cGMP-dependent kinase is unlikely to mediate the response. The effects of the other agents also support the similarities in pharmacology between AQP1 and the CNG channels, in that 8pCPT-cGMP is an activator of both cGMP-gated ion channels and of the ionic current in AQP1-expressing oocytes, whereas Rp-8-Br-PET-cGMPS is an inhibitor of both retinal cGMP-gated ion channels and of the ionic conductance in AQP1-expressing oocytes.

In sum, the results presented here support the conclusion that the cGMP-stimulated ionic conductance arises from AQP1 channels, is activated by direct binding of cGMP to the AQP1 channel, and cannot be mimicked by the expression of another water-conducting member of the MIP family that lacks the same degree of sequence homology for amino acids in the putative cyclic nucleotide-binding region of the carboxyl terminus.

Discussion

AQP1 channels are not strictly dedicated to water transport. Expression of AQP1 channels has been shown to enhance membrane permeability to small molecules such as carbon dioxide (Nakhoul et al., 1998), glycerol (Abrami et al., 1995), and cations (Yool et al., 1996), although an ion channel function for AQP1 has been disputed (Yasui et al., 1999). Data presented here provide several new lines of evidence that AQP1 channels do carry an ionic current. Sequence homology with CNG channels suggests a putative cyclic nucleotide-binding site in the carboxyl terminal domain of AQP1. A direct action of cGMP binding in activating an ionic conductance through AQP1 channels is suggested by four lines of evidence.

First, the pretreatment of AQP1-expressing oocytes with H7 has no discernible effect on the conductance response to cGMP, indicating that the involvement of an H7-sensitive kinase is not required. In contrast, we showed previously

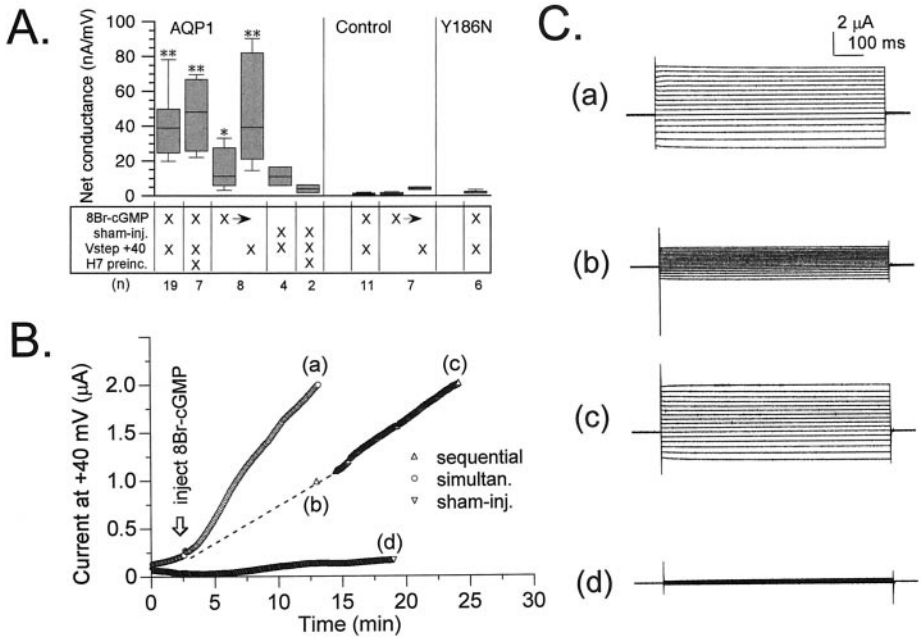

Fig. 6. Summary of the effects of 8-Br-cGMP and depolarization on the net conductance responses of AQP1 wild-type, AQP1 Y186N mutant, and control oocytes, measured by two-electrode voltage-clamp recordings. A, net conductances (μS) were determined 10 min after the injection of 8-Br-cGMP (50 nl of 100 mM) or equivalent sham injections. The matrix summarizes the treatment conditions. Vstep +40, that the membrane potential was stepped for 800 ms to +40 mV once every 5 s throughout the recording. H7 preinc, the oocytes were pretreated 2 to 4 h with 10 μM H7, which also was present in the recording saline. X→, after 8-Br-cGMP injection, the oocyte was held for 10 min at −40 mV until the first net conductance measurement, followed by 10 min of +40-mV voltage steps until the second conductance measurement (sequential paradigm). Conductance values were calculated from linear fits of the current-voltage relationships. Boxes show 50% of data points, error bars show the range of data, and horizontal bars indicate median values. Data are mean ± S.E., with (n) for numbers of oocytes. *Statistically significant differences from controls (*$P < .05$, **$P < .01$, nonparametric Mann–Whitney test). Control oocytes showed no ionic current response to 8-Br-cGMP injection and depolarization. B, comparison of the rates of activation of ionic current in AQP1-expressing oocytes subjected either to simultaneous stimulation with 8-Br-cGMP and depolarization or to sequential stimulation first with 8-Br-cGMP at −40 mV, followed by the application of the depolarization step protocol. Sham-injection of AQP1-expressing oocytes (with depolarizing steps) evoked little response. C, net current responses to a set of voltage steps illustrate the currents sampled at time points (a) to (d) in B. Voltage steps were +60 mV to −80 mV in −10-mV intervals, from −40 mV holding potential.

that H7 pretreatment inhibited the current response to cAMP as well as to the catalytic subunit of PKA (Yool et al., 1996), thus showing that the action of cAMP in activating ionic conductance in AQP1-expressing oocytes is indirectly mediated by a signal cascade involving protein kinase activity. Pharmacological analyses support the similarities between general mechanisms of direct activation and block of CNG channels and of the ionic conductance seen in AQP1-expressing oocytes.

Second, inside-out patches excised from AQP1-expressing oocytes showed sustained activity of unique large conductance ion channels after application of cGMP. Channel activation in an excised patch provides evidence for direct cGMP regulation; involvement of a membrane-associated kinase in the channel activation process is unlikely because ATP was not included in the bath saline. The cGMP-activated channels show long open times and a high unitary conductance that distinguish them from endogenous ion channels of *X.*

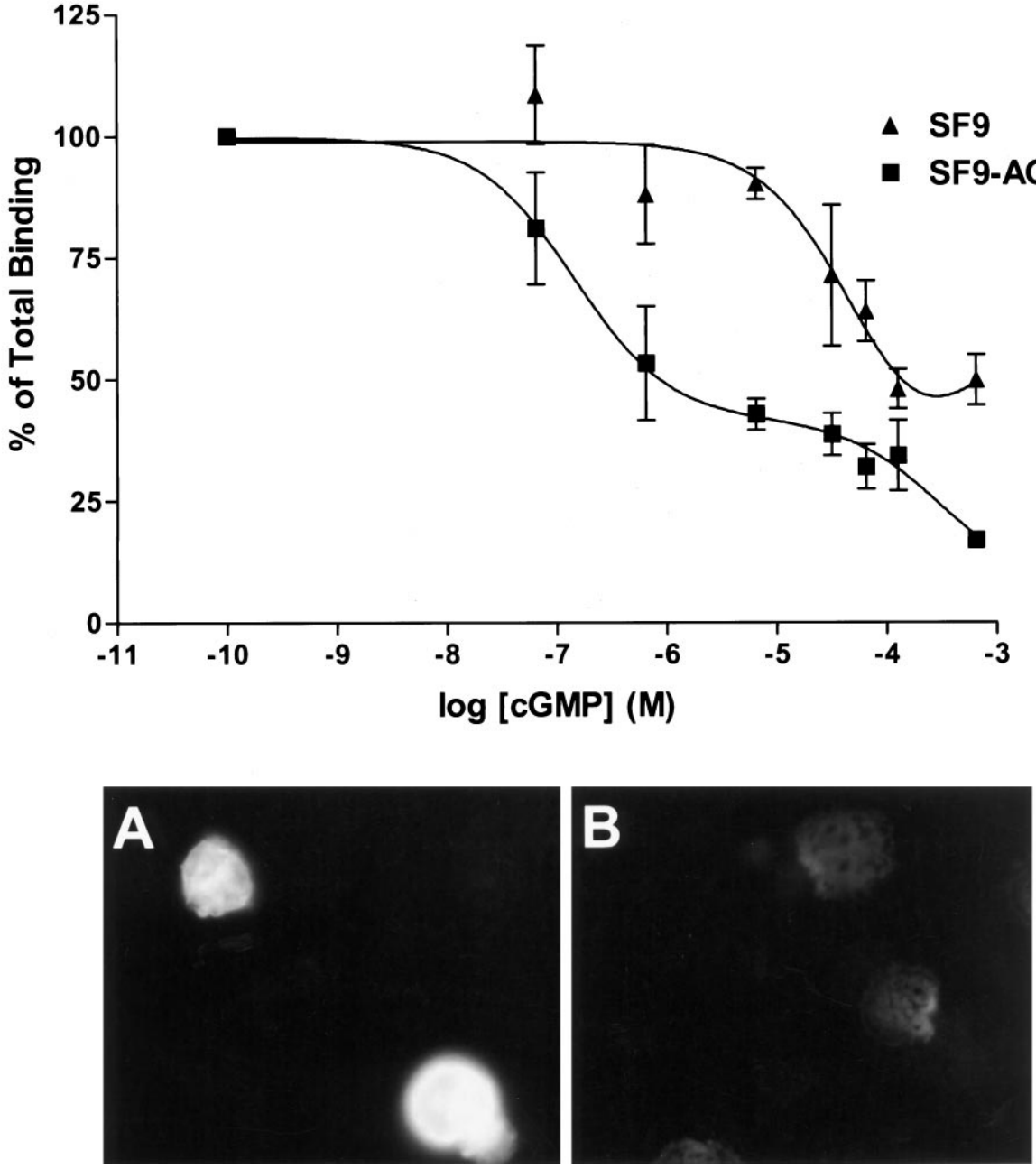

Fig. 7. Expression of AQP1 in Sf9 cells, analyzed by radioligand binding with [^{3}H]cGMP and immunofluorescence labeling with antibodies to AQP1. The graph shows the binding of [^{3}H]cGMP in membranes from Sf9 cells infected with recombinant baculovirus encoding AQP1 (■) or with recombinant baculovirus alone (▲). Binding was performed as described in *Materials and Methods* with a final concentration of 0.6 μM [^{3}H]cGMP and the indicated concentrations of unlabeled cGMP. Incubations were made for 30 min on ice followed by centrifugation to separate bound and free [^{3}H]cGMP. Nonlinear regression analysis for one-site competition (Prism) yielded a K_D value of 0.2 ± 0.2 μM (mean ± S.E.) for AQP1-expressing membranes and 27.1 ± 0.3 μM for the control membranes. Data shown are mean ± S.E. from three separate experiments. Bottom, AQP1-like immunoreactivity in Sf9 cells infected with recombinant baculovirus encoding human AQP1 (A) but not in Sf9 cells infected with recombinant baculovirus alone (B). Antibodies were generated against a GST/AQP1 fusion peptide as described previously (Stamer et al., 1995) and were labeled with secondary antibody (see *Materials and Methods*).

laevis oocytes. The doses of cGMP used in the excised-patch studies (~0.1 mM) were approximately 500-fold greater than the estimated K_D value for cGMP binding in AQP1 and thus may be above saturating levels. Before carrying out more precise dose-response studies, it will be necessary to understand the influence of other factors (e.g., voltage) on the magnitude and time course of the AQP1 conductance response.

Third, binding studies with membranes from AQP1-infected Sf9 cells showed a high-affinity binding component with [^{3}H]cGMP that was not present in control Sf9 cells. These results suggested that a cGMP-binding site, conferred by expression of AQP1, could mediate the ionic conductance effects that we have observed. Interestingly, similar cGMP binding was found in red blood cells (Boadu and Sager, 1997), which are known to express high levels of AQP1 (King and Agre, 1996). In fact, the binding affinity of the red blood cell cGMP-binding protein (K_D = 0.16 μM) was similar to the value we obtained in the present study (K_D = 0.2 μM).

Fourth, oocytes expressing AQP5 showed no ionic conductance response to the injection of cGMP. AQP5 has less sequence homology with CNG channels in the carboxyl-terminal domain than does AQP1. Current amplitudes of AQP5-expressing oocytes were indistinguishable from those of control oocytes throughout the duration of two-electrode voltage-clamp recordings, regardless of depolarization and 8-Br-

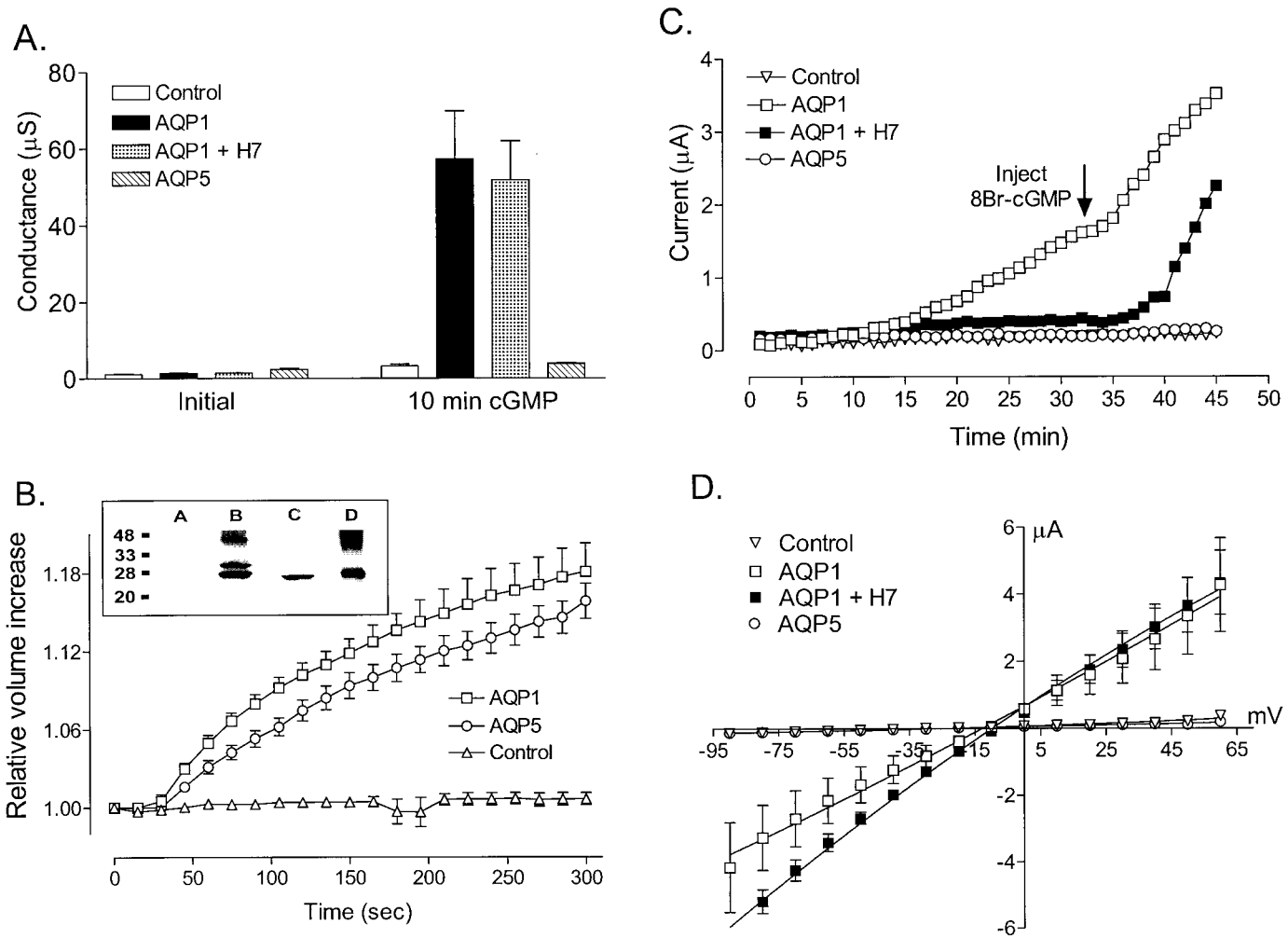

Fig. 8. Comparison of ionic and osmotic water permeabilities in oocytes expressing AQP1 or AQP5 channels and control oocytes harvested from the same batch. A, summary of conductance values (mean ± S.E.) measured before (Initial) and 10 min after injection of 50 nl of 100 mM 8-Br-cGMP (10 min cGMP), with the depolarizing step protocol (800-ms steps to +40 mV from a holding potential of −40 mV, repeated every 5 s) during two-electrode voltage-clamp recordings. Control oocytes (open columns, n = 3) and AQP5-expressing oocytes (diagonally striped columns, n = 3) showed no 8-Br-cGMP-induced response. AQP1-expressing oocytes were either untreated (filled columns; n = 3) or preincubated in 10 μM H7 for 2 h (dotted columns, n = 2); both groups showed an ionic conductance in response to 8-Br-cGMP injection. B, swelling assays (graph) and Western blot (inset) confirmed the expression of functional AQP1 and AQP5 channels in the same batch of oocytes. Relative volume increases were measured with reference to initial oocyte volume (set as 1.00) and plotted as a function of time after the introduction of oocytes into 100 mOsM hypotonic saline at time zero. Oocytes expressing AQP1 (□) or AQP5 (○) showed comparable rates of swelling. Control oocytes (△) showed no appreciable volume change. Data shown are mean ± S.E. for five oocytes per group. Western blot analysis (inset) with subtype-specific antibodies against the carboxyl terminals confirmed the expression of AQP1 and AQP5 proteins at expected sizes (kDa) in membranes isolated from the same batch of oocytes used for data shown in A. Lane 1, control oocytes; lane 2, AQP1-expressing oocytes; lane 3, AQP5-expressing oocytes; and lane 4, red blood cells (native AQP1). C, data show the current amplitudes measured at repetitive steps to +40 mV, plotted as a function of time. Holding potential was −40 mV. All oocytes were injected with 8-Br-cGMP at the time indicated by the arrow. Spontaneous activation of the AQP1 current before 8-Br-cGMP injection (□) was blocked by 10 μM H7 (■). AQP5-expressing (○) and control oocytes (▽) showed no response to 8-Br-cGMP injection with depolarizing steps. Final conductance levels beyond 45 min reached comparable magnitudes in AQP1-expressing oocytes with or without H7. D, net conductance responses of AQP1, AQP5, and control oocytes to 8-Br-cGMP, after the depolarization step protocol. Data shown are mean ± S.E.

cGMP injection. These results demonstrated that the ionic conductance response seen for AQP1-expressing oocytes cannot be attributed simply to an up-regulation of endogenous oocyte ion channels as a result of increased membrane water permeability. Similarly, the lack of an ionic conductance response with the nonfunctional mutant Y1986N served as a control that ruled out a hypothetical effect of the physical presence of AQP1 protein itself on oocyte plasma membrane conduction properties.

AQP1 channels are similar to the CNG channels of sensory cells (Zagotta and Siegelbaum, 1996) in their subunit transmembrane structure and tetrameric organization (King and Agre, 1996); in having a nonselective cationic permeability (Yool et al., 1996); in being activated by direct cyclic nucleotide binding, probably to a site in the carboxyl tail domain; and in their pharmacological sensitivities to agonists and antagonists. At the onset of activation of AQP1 channels by cGMP, we noted that the channels appear to go through a mode consisting of flickery bursts of openings before shifting into the long opening mode of channel activity. In retinal CNG channels expressed in oocytes, flickery opening behavior of CNG channels and subconductance states have been associated with the level of occupancy of binding sites by ligand, with maximal channel opening dependent on having all four sites in the tetramer bound (Ruiz and Karpen, 1999). It is possible that the fully open channel mode for AQP1 channels described here may similarly reflect a state in which all four binding sites are occupied by cGMP. In CNG channels, the rate of activation by cyclic nucleotide is primarily diffusion-limited (Karpen et al., 1988). Our single-channel recordings showed that the AQP1 channels took minutes to activate after cGMP application to the inside face of the patch. This unusual delay may indicate that another factor (e.g., a rate-limiting conformational change that is in part voltage-dependent) might affect cGMP binding or opening of AQP1 channels. These observations of both similarities and differences between AQP1 and CNG channels provide intriguing areas for further studies.

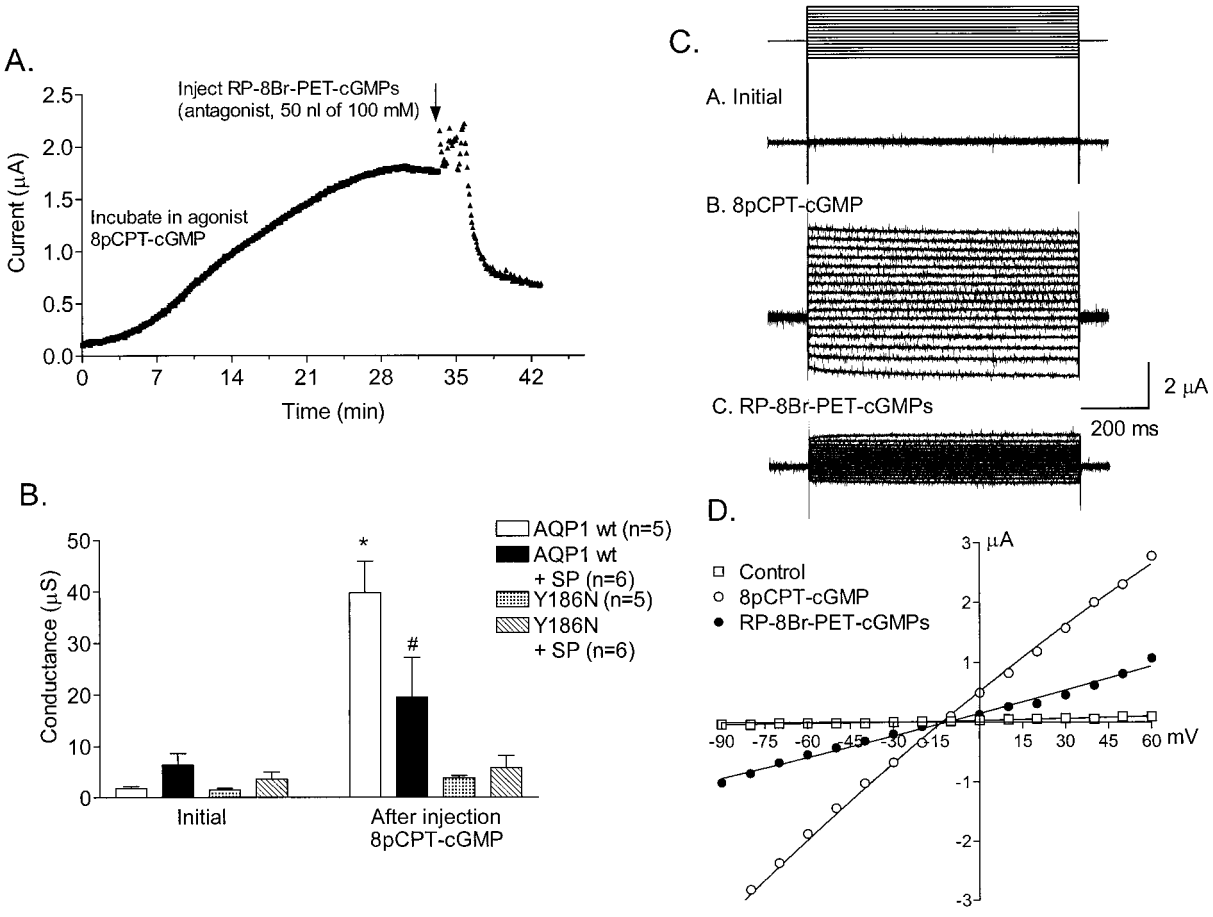

Fig. 9. Pharmacological properties of AQP1 ionic conductance activation and block. A, block of the AQP1 ionic current by on-line injection (arrow) of the CNG channel antagonist Rp-8-Br-PET-cGMPS (50 nl of 100 mM). AQP1-expressing oocytes were preincubated 15 min in membrane-permeant agonist 8pCPT-cGMP (10 mM). The agonist remained present in the bath during recording. Current was monitored with 0.8-s steps to +40 mV every 5 s, starting at time zero. Comparable responses were obtained in duplicate experiments. B, impaired activation of AQP1 wild-type (wt) current after 15-min preincubation with antagonist Sp-8-Br-PET-cGMPS (10 μM SP). For preincubated oocytes, the antagonist was maintained in the recording bath saline as well. Current was measured at 10 min after injection of agonist 8pCPT-cGMP (50 nl of 100 mM). Nonfunctional AQP1 mutant (Y186N) was expressed in plasma membrane but conferred no response to cGMP agonist. *Significant difference for AQP1 wild type between the initial condition and the response after the injection of 8pCPT-cGMP, without SP pretreatment ($P < .05$). #Significant difference between SP-treated and untreated AQP1 wild-type responses to 8pCPT-cGMP injection ($P < .05$). C, traces for three time points during the recording shown in A. Initial, at time zero, after 15-min preincubation. 8pCPT-cGMP, at the time of the peak development of the response (at recording time ~31 min). RP-8-Br-cGMPS, after the injection of the antagonist (at recording time ~42 min). The voltage was stepped from +60 to −90 in 10-mV increments from a holding potential of −40 mV (shown at top). D, current-voltage relationships for data in C. Comparable block by Rp-8-Br-PET-cGMPs was observed in duplicate experiments.

The open probability of the AQP1 channel showed sensitivity to voltage, in that depolarized potentials promoted the fully open mode in the presence of cGMP, whereas hyperpolarized potentials decreased channel open probability and produced shorter bursts of channel events that would appear to account for the decay phase seen in the ensemble averaged currents. In contrast, two-electrode voltage-clamp recordings showed little evidence for a decay phase for the inward current at hyperpolarized potentials. In fact, in many oocytes, the inward current at strongly hyperpolarized potentials showed a slowly activating increase (rather than a decrease) in amplitude that could reflect an added contribution from the slow hyperpolarization-activated endogenous oocyte current described previously (Tzounopoulos et al., 1995). Alternatively, the difference between the whole-cell currents and the ensemble averaged currents at hyperpolarized potentials may reflect a difference between the properties of AQP1 channels located in the intact membrane as opposed to being in the excised-patch environment, including factors such as bath saline composition or altered protein interactions with intracellular components such as cytoskeleton or modulatory agents. CNG channels of olfactory epithelia show voltage-dependent block by external divalent cations that increases with hyperpolarization (Zufall and Firestein, 1993); this phenomenon also may provide insight into the mechanism that induces transient activity of AQP1 channels at hyperpolarized potentials.

The spontaneous activation of ionic conductance, seen in some batches of AQP1-expressing oocytes, involves endogenous signaling and is blocked by preincubation of oocytes in H7, whereas the inductive action of cGMP agonists is unaffected by the kinase inhibitor. The spontaneous activation may result from basal levels of PKA activity in oocytes. The link between PKA and cGMP in the stimulation of AQP1 ionic conductance is not yet known and could include an number of possibilities, such as phosphorylation of AQP1 at an atypical consensus site, phosphorylation of a protein associated with AQP1 channels, or enhancement of endogenous cGMP levels by regulation of guanylate cyclase or phosphodiesterase. The similar magnitudes of the final amplitudes of current in AQP1-expressing oocytes, whether achieved by cGMP stimulation alone or by a combination of spontaneous activation and cGMP, suggest that the maximal current response level is set by the total population of AQP1 channels expressed in the membrane. CNG channels are known to be modulated by Ca^{2+}, Ca^{2+}-calmodulin, phosphorylation, diacylglycerol analogs, and divalent cations (Zagotta and Siegelbaum, 1996; Molokanova et al., 1997). It would seem likely that intracellular signaling could modulate ion channel function of AQP1 as well.

The ion-conducting channels identified thus far in the MIP family (AQP1, AQP6, lens MIP, and Nod26) show regions of amino acid identity within the putative pore-forming regions, loop B (the S1–S2 linker) and loop E (the S5–S6 linker), that are also seen in other aquaporins (Agre et al., 1993). A unique sequence of three amino acids, NPA, is found in both loops in most members of the MIP family. Loop E in AQP1 forms part of the water pore and contains a cysteine-binding site for the pore-blocking compound mercury (Preston et al., 1993). Loop B contains a lysine residue that affects ion selectivity in AQP6 channels (Yasui et al., 1999). Mutation of the S6 domain in the insect aquaporin, AQPcic, alters the relative permeabilities of water and glycerol (Lagrée et al., 1999). The broader family of ion channels (K^+ channels, CNG channels, and other voltage-gated channels) contains pore-lining sequences in the S5–S6 loops, with the pore formed in the center of the tetramer of subunits (Jan and Jan, 1992). These features suggest interesting similarities between functional domains of aquaporins and other ion channels. However, in aquaporins, it has been suggested that each subunit of the tetrameric channel forms an independent pore for water movement (Agre et al., 1993). The location of the ionic pore in AQP1 remains unknown, but similarities with CNG and K^+ channels would suggest that a central pore for ions is a reasonable hypothesis. Whether water and ions move through the same pore or parallel conduction pathways in AQP1 remains to be determined.

AQP1 is expressed in many tissues (King and Agre, 1996) in which an elevation of cGMP could in theory contribute to AQP1 channel regulation. Previously unrecognized clues to the function of AQP1 as a cGMP-gated ion channel may exist in the published literature (e.g., Darvish et al., 1995; Stumpff et al., 1997). Work presented here addresses fundamental properties of an important class of membrane channels whose physiological significance is just beginning to be appreciated. Our work showing an ionic signaling capacity in AQP1 channels identifies a new avenue of research that merits further investigation. It is now imperative to determine whether the ion channel functions for AQP1 and AQP6 that have been described using the *X. laevis* oocyte expression system can be confirmed in native cells expressing these channels. Insights into clinical applications may take advantage of the presence of cGMP-coupled receptors for manipulating transmembrane transport processes in tissues that express AQP1 channels. Basic research on functional domains of AQP1 channels will provide the foundation needed to dissect the signaling pathways that are involved in the physiological regulation of AQP1 channel function. Reevaluation of a possible role in signaling may not be limited to AQP1; it is possible that other members of the MIP family may also be found to carry ion currents when activated by an appropriate stimulus.

Acknowledgments

We thank Drs. Kurt Beam, James Hall, Jeffrey Karpen, and William Zagotta for helpful discussions.

References

Abrami L, Tacnet F and Ripoche P (1995) Evidence for a glycerol pathway through aquaporin1 (CHIP28) channels. *Pfluegers Arch* **430:**447–458.
Agre P, Lee MD, Devidas S and Guggino WB (1997) Aquaporins and ion conductance. *Science (Wash DC)* **275:**1490.
Agre P, Preston GM, Smith BL, Jung JS, Raina S, Moon C, Guggino WB and Nielsen S (1993) Aquaporin CHIP: The archetypal molecular water channel. *Am J Physiol* **265:**F463–F476.
Boadu E and Sager G (1997) Binding characterization of a putative cGMP transporter in the cell membrane of human erythrocytes. *Biochemistry* **9:**10954–10958.
Bradley J, Li J, Davidson N, Lester HA and Zinn K (1994) Heteromeric olfactory cyclic nucleotide-gated channels: A new subunit that confers increased sensitivity to cAMP. *Proc Natl Acad Sci USA* **91:**8890–8894.
Brooks H, Regan JW and Yool AJ (2000) Inhibition of Aquaporin-1 water permeability by TEA: Involvement of the loop E pore region. *Mol Pharmacol,* in press.
Darvish N, Winaver J and Dagan D (1995) A novel cGMP-activated Cl^- channel in renal proximal tubules. *Am J Physiol* **268:**F323–F329.
Deen PMT, Mulders SM, Kansen SM and van Os CH (1997) Aquaporins and ion conductance. *Science (Wash DC)* **275:**1491.
Dhallan RS, Yau KW, Schrader KA and Reed RR (1990) Primary structure and functional expression of a cyclic nucleotide-activated channel from olfactory neurons. *Nature (Lond)* **347:**184–187.
Ehring GR, Zampighi G, Horwitz J, Bok D and Hall JE (1990) Properties of channels

reconstituted from the major intrinsic protein of lens fiber membranes. *J Gen Physiol* **96:**631–664.
Fischbarg J, Kuang K, Li J, Iserovich P and Wen Q (1997) Aquaporins and ion conductance. *Science (Wash DC)* **275:**1491–1492.
Goulding EH, Ngai J, Kramer RH, Colicos S, Axel R, Siegelbaum SA and Chess A (1992) Molecular cloning and single channel properties of the cyclic nucleotide-gated channel from catfish olfactory neurons. *Neuron* **8:**45–58.
Goulding EH, Tibbs GR and Siegelbaum SA (1994) Molecular mechanism of cyclic-nucleotide-gated channel activation. *Nature (Lond)* **372:**369–374.
Jan LY and Jan YN (1992) Structural elements involved in specific K^+ channel functions. *Annu Rev Physiol* **54:**537–555.
Karpen JW, Zimmerman AL, Stryer L and Baylor DA (1988) Gating kinetics of the cyclic-GMP-activated channel of retinal rods: Flash photolysis and voltage-jump kinetics. *Proc Natl Acad Sci USA* **85:**1287–1291.
Kaupp UB, Niidome T, Tanabe T, Terada S, Boenigk W, Stuehmer W, Cook NJ, Kangawa K, Matsuo H, Hirose T, Miyata T and Numa S (1989) Primary structure and functional expression from complementary DNA of the rod photoreceptor cyclic GMP- gated channel. *Nature (Lond)* **342:**762–766.
King LS and Agre P (1996) Pathophysiology of the aquaporin water channels. *Annu Rev Physiol* **58:**619–648.
Lagrée V, Froger A, Deschamps S, Hubert J-F, Delamarche C, Bonnec G, Thomas D, Gouranton J and Pellerin I (1999) Switch from an aquaporin to a glycerol channel by two amino acids substitution. *J Biol Chem* **274:**6817–6819.
Miledi R and Woodward RM (1989) Effects of defolliculation on membrane current responses of *Xenopus* oocytes. *J Physiol* **416:**601–621.
Molokanova E, Trivedi B, Savchenko A and Kramer RH (1997) Modulation of rod photoreceptor cyclic nucleotide-gated channels by tyrosine phosphorylation. *J Neurosci* **17:**9068–9076.
Mulders SM, Preston GM, Deen PMT, Guggino WB, van Os CH and Agre P (1995) Water channel properties of major intrinsic protein of the lens. *J Biol Chem* **270:**9010–9016.
Nakhoul NL, Davis BA, Romero MF and Boron WF (1998) Effect of expressing the water channel aquaporin-1 on the CO_2 permeability of *Xenopus* oocytes. *Am J Physiol* **274:**C543–C548.
Patil RV, Han Z and Wax MB (1997a) Regulation of water channel activity of aquaporin 1 by arginine vasopressin and atrial natriuretic peptide. *Biochem Biophys Res Commun* **238:**392–396.
Patil RV, Han Z and Wax MB (1997b) Aquaporins and ion conductance. *Science (Wash DC)* **275:**1492.
Preston GM and Agre P (1991) Isolation of the cDNA for erythrocyte integral membrane protein of 28 kilodaltons: Member of an ancient channel family. *Proc Natl Acad Sci USA* **88:**11110–11114.
Preston GM, Carroll TP, Guggino WB and Agre P (1992) Appearance of water channels in *Xenopus* oocytes expressing red cell CHIP28 protein. *Science (Wash DC)* **256:**385–387.
Preston GM, Jung JS, Guggino WB and Agre P (1993) The mercury-sensitive residue at cysteine 189 in the CHIP28 water channel. *J Biol Chem* **268:**17–20.
Raina S, Preston GM, Guggino WB and Agre P (1995) Molecular cloning and characterization of an aquaporin cDNA from salivary, lacrimal, and respiratory tissue. *J Biol Chem* **270:**1908–1912.
Ruiz ML and Karpen JW (1999) Opening mechanism of a cyclic nucleotide-gated channel based on analysis of single channels locked in each liganded state. *J Gen Physiol* **113:**873–895.
Smith AA, Brooker T and Brooker G (1987) Expression of rat mRNA coding for hormone-stimulated adenylate cyclase in *Xenopus* oocytes. *FASEB J* **1:**380–387.
Stamer WD, Seftor REB, Snyder RW and Regan JW (1995) Cultured human trabecular meshwork cells express aquaporin-1 water channels. *Curr Eye Res* **14:**1095–1100.
Stumpff F, Strauss O, Boxberger M and Wiederholt M (1997) Characterization of maxi-K-channels in bovine trabecular meshwork and their activation by cyclic guanosine monophosphate. *Invest Ophthal Vis Sci* **38:**1883–1892.
Tzounopoulos T, Maylie J and Adelman JP (1995) Induction of endogenous channels by high levels of heterologous membrane proteins in *Xenopus* oocytes. *Biophys J* **69:**904–908.
Varnum MD, Black KD and Zagotta WN (1995) Molecular mechanism for ligand discrimination of cyclic nucleotide-gated channels. *Neuron* **15:**619–625.
Weaver CD, Shomer NH, Louis CF and Roberts DM (1994) Nodulin 26, a nodule-specific symbiosome membrane protein from soybean, is an ion channel. *J Biol Chem* **269:**17858–17862.
Yasui M, Hazama A, Kwon T-H, Nielsen S, Guggino WB and Agre P (1999) Rapid gating and anion permeability of an intracellular aquaporin. *Nature (Lond)* **402:**184–187.
Yool AJ, Stamer WD and Regan JW (1996) Forskolin stimulation of water and cation permeability in aquaporin 1 water channels. *Science (Wash DC)* **273:**1216–1218.
Zagotta WN and Siegelbaum SA (1996) Structure and function of cyclic nucleotide-gated channels. *Annu Rev Neurosci* **19:**235–263.
Zufall F and Firestein S (1993) Divalent cations block the cyclic nucleotide-gated channel of olfactory receptor neurons. *J Neurophysiol* **69:**1758–1768.

Send reprint requests to: Andrea Yool, Ph.D., Department of Physiology, P.O. Box 24-5051, University of Arizona College of Medicine, Tucson, AZ 85724-5051. E-mail: ayool@u.arizona.edu